

Cyclin B1 expression as an independent prognostic factor for lung adenocarcinoma and its potential pathways

YI LI^{1*}, YUANXIU LENG^{2*}, YUDI DONG¹, YONGXIANG SONG³, QIAOYUAN WU¹,
NI JIANG¹, HUI DONG¹, FANG CHEN¹, QING LUO¹ and CHEN CHENG³

¹Department of Cancer Research Laboratory, Department of Pathology, Affiliated Hospital of Zunyi Medical University, Zunyi, Guizhou 563003; ²Department of Oncology, Guihang Guiyang Hospital, Guiyang, Guizhou 550000;

³Department of Thoracic Surgery, Affiliated Hospital of Zunyi Medical University, Zunyi, Guizhou 563003, P.R. China

Received March 15, 2022; Accepted August 26, 2022

DOI: 10.3892/ol.2022.13561

Abstract. Although great progress has been made in the early diagnosis and targeted therapy of lung adenocarcinoma (LUAD), the survival of patients with LUAD remains unsatisfactory. There is an urgent requirement for new biomarkers to guide the diagnosis, prognosis and treatment of LUAD. Following an initial bioinformatics screen, the present study focused on cyclin B1 (CCNB1) in LUAD. A total of 94 patients with LUAD from a single hospital were included in the study. CCNB1 protein expression was detected and scored in 94 LUAD samples and 30 normal tissue samples by immunohistochemistry. The associations between CCNB1 expression and the clinicopathological features of the patients with LUAD were analyzed. Furthermore, the relationship between prognosis and the CCNB1 expression level was analyzed using Cox regression and survival analyses. Weighted gene co-expression network analysis and RNA-sequencing were also applied to identify the potential molecular mechanisms of CCNB1 in LUAD. CCNB1 was highly expressed in patients with LUAD and was associated with poor prognosis. It may affect the expression of CPLX1, PPIF, SRPK2, KRT8, SLC20A1 and CBX2 genes and function via different pathways. CCNB1 has the potential to become a novel prognostic target for LUAD.

Introduction

Lung cancer is the most common malignancy with the highest mortality rate worldwide (1). There are two main histopathological types of lung cancer: Non-small cell lung cancer (NSCLC) and small cell lung cancer (2). Lung adenocarcinoma (LUAD) is one of the most frequently occurring types of NSCLC and accounts for approximately half of all lung cancers (3). Despite advancements in early diagnosis and targeted therapies, the prognosis of patients with LUAD remains unsatisfactory, and the 5-year survival rate is <25% (4). New treatment strategies are required to improve the clinical outcomes of patients with LUAD, particularly those diagnosed with unresectable, locally advanced or metastatic LUAD. Therefore, it is urgently necessary to explore the molecular mechanisms of LUAD to further understand this disease and discover novel biomarkers for its diagnosis, prognosis and treatment.

Cyclins are proteins that bind to cyclin-dependent kinases (CDKs) and thereby regulate the cell division cycle (5,6); the HUGO Gene Nomenclature Committee lists 31 members in the cyclin gene group (7). Cyclin B1 (CCNB1) is considered as a mitotic cyclin, which plays a key role in the regulation of CDK1 by complexing with it to promote the transition of the cell cycle from the G2 phase to mitosis (8). In the metaphase and late stages of mitosis, degradation of CCNB1 occurs through the ubiquitin proteasome pathway, leading to chromosome depolymerization and nucleolar and nuclear membrane regeneration (9). Previous studies have demonstrated that CCNB1 is abnormally expressed in a variety of tumors and is associated with poor prognosis (10-12). A study by Gu *et al* (13) evaluated the upregulation of CCNB1 in liver cancer tissues compared with normal liver tissues, and found that a high expression level of CCNB1 was closely associated with poor prognosis in patients with hepatocellular carcinoma (HCC). Furthermore, the study demonstrated that the knockdown of CCNB1 significantly inhibited the proliferation, migration and invasion of HCC cells. Another study reported that CCNB1 was upregulated in colorectal cancer tissues and negatively associated with lymph node metastasis, distant metastasis and TNM stage, and the survival rate of patients with higher CCNB1 expression was significantly higher than that of patients with lower CCNB1 expression. In addition, cell-based experiments

Correspondence to: Dr Qing Luo, Department of Cancer Research Laboratory, Department of Pathology, Affiliated Hospital of Zunyi Medical University, 149 Dalian Road, Huichuan, Zunyi, Guizhou 563003, P.R. China
E-mail: zlsyuloqing@163.com

Dr Chen Cheng, Department of Thoracic Surgery, Affiliated Hospital of Zunyi Medical University, 149 Dalian Road, Huichuan, Zunyi, Guizhou 563003, P.R. China
E-mail: 29217036@qq.com

*Contributed equally

Key words: cyclin B1, lung adenocarcinoma, survival, RNA-sequencing, weighted gene coexpression-analysis, biomarker

in the study revealed that the inhibition of CCNB1 expression increased the migration and invasion of colorectal cancer cells (14). Therefore, CCNB1 may be a prognostic biomarker. In addition, cancers are associated with increased inflammatory burden. Numerous studies have shown an association between inflammatory markers and malignant conditions (15). Also, a recent study has demonstrated that CCNB1 is involved in atherosclerosis-induced inflammation in blood vessels (16). Therefore, the expression of CCNB1 in cancer is worthy of evaluation.

A study revealed that in lung cancer, the CCNB1 expression level is upregulated and higher levels of CCNB1 indicate poorer survival outcomes (17). Mechanistically, the degradation of CCNB1 by anaphase promoting complex subunit 11 via ubiquitin-60S ribosomal protein L49 ubiquitylation is critical in the cell cycle progression and proliferation of NSCLC cell lines (18). In another study, CCNB1 overexpression was shown to promote the progression of LUAD cells, and it was suggested that microRNA-139-5p negatively regulates CCNB1 in LUAD, thereby suppressing cell proliferation, migration, invasion and the cell cycle (19).

However, the clinical characteristics of CCNB1 in lung cancer, particularly LUAD, remain unclear, and its potential mechanism requires further exploration. Therefore, in the present study, the expression of CCNB1 in LUAD was analyzed and its association with the clinicopathological features and prognosis of patients with LUAD was explored. Furthermore, the molecular mechanism of CCNB1 and its use in the prognosis of LUAD were preliminarily investigated.

Materials and methods

Data mining. The RNA-sequencing (RNA-seq) data and clinical data of 535 LUAD samples and 59 normal samples were downloaded from The Cancer Genome Atlas (TCGA; <https://portal.gdc.cancer.gov/>). After the exclusion of those samples without completely specific TNM stage and intact survival data, 334 LUAD samples were finally used in the present study. The clinicopathological data were downloaded for reanalysis, including the age at the initial diagnosis, sex, clinical stage, TNM stage, survival status and overall survival time. The RNA-seq data of LUAD were also downloaded from the Gene Expression Omnibus (GEO) database (www.ncbi.nlm.nih.gov/geo) for analysis of the transcription level of CCNB1 (GSE116959; 11 healthy lung and 57 LUAD samples; <https://www.ncbi.nlm.nih.gov/geo/query/acc.cgi?acc=GSE116959>) (20). All samples were divided into low and high expression groups according to the median value of CCNB1 expression.

Kyoto encyclopedia of genes and genomes (KEGG) and gene ontology (GO) enrichment analyses. Pathway enrichment analysis of differential genes (DEGs) was performed using the KEGG (<https://www.kegg.jp/>) and GO databases (<http://geneontology.org/docs/ontology-documentation/>). KEGG combines numerous database resources from high-throughput experimental technologies at the molecular level, while the GO database is widely used in bioinformatics to provide information on cellular components (CC), molecular functions (MF) and biological processes (BP). The Org.Hs.eg.db R package

(version 3.6.0; <https://bioconductor.org/packages/org.Hs.eg.db/>) was used to convert the symbols of DEGs into Entrez IDs. Subsequently, KEGG analysis was performed using the enrichKEGG function of the clusterProfiler R package (version 3.6.0; <https://bioconductor.org/packages/clusterProfiler/>). GO analysis was performed using the enrichGO function in clusterProfiler. The results of the KEGG and GO enrichment analyses were visualized using the ggplot2 R package (version 3.3.5; <https://ggplot2.tidyverse.org>).

Weighted gene co-expression network analysis (WGCNA). WGCNA involves the construction of a weighted gene expression network that represents the associations between different genes and can be used to identify highly coordinated gene sets. In the present study, the expression data of the DEGs were used to construct a gene co-expression network using the WGCNA R package (version 3.6.0; <http://horvath.genetics.ucla.edu/html/CoexpressionNetwork/Rpackages/WGCNA/>). The DEGs for the WGCNA were screened using edgeR (version 3.6.0; <https://bioconductor.org/packages/edgeR/>) (defined as fold change ≥ 1 and $P \leq 0.05$). The WGCNA included identification of the gene expression similarity matrix, adjacency matrix and co-expression network. A scale-free plot was used to evaluate whether the network exhibited a scale-free topology. The power value of the soft threshold of the adjacency matrix was set as 5 to meet the scale-free topology criterion. The hierarchical clustering analysis was based on the average linkage generated by a dynamic analysis using the tree-cut method for branch cutting (cut height, 0.995; minimum cluster size, 30).

Patient inclusion criteria and tissue sample collection. LUAD tissue samples were collected from 94 patients undergoing surgical resection in the Department of Thoracic Surgery of the Affiliated Hospital of Zunyi Medical University (Zunyi, China) between January 2010 and August 2015. The patients included 54 females and 40 males. The oldest was 76 years old and the youngest was 21 years old, and the media age was 57 years. Due to the collection of normal lung tissue being challenging, and paracancerous tissue being different from normal tissue and potentially having different biological properties, an independent normal lung tissue series was used as a control for the institutional LUAD tissues (21). This comprised 30 normal lung tissue sections, which were purchased from Shanghai Xinchao Biological Technology Co., Ltd. The following criteria were met in all cases: i) Histologically diagnosed LUAD; ii) complete clinical data; and iii) no other malignant tumor was present and the patients did not accept tumor-related treatment before the initial diagnosis, such as radiotherapy, chemotherapy and immunotherapy. Tissue samples were fixed in 4% paraformaldehyde and then embedded in paraffin for postoperative immunohistochemistry. The pathological stage was determined according to the Union for International Cancer Control and American Joint Committee on Cancer staging criteria (eighth edition). The follow-up was initiated on the day of surgery and terminated in January 2019 or at death. Overall survival (OS) was defined as the interval from the end of surgery to the date of the last follow-up or death. This study obtained written consent from all patients and was approved by the Research Ethics Committee of the Affiliated Hospital of Zunyi Medical University [no. (2021)1-098].

Immunohistochemistry (IHC). The LUAD tumor tissues were fixed in 4% paraformaldehyde for 24 h at room temperature, dehydrated with graded ethanol and cleared with xylene. After embedding in paraffin, the tumor tissues were sectioned into 4- μ m slices. The paraffin sections were dewaxed with xylene and hydrated with gradient ethanol using standard procedures. After treatment with citrate buffer (pH 6.0) for antigen retrieval at 95°C for 12 min, the slices were incubated with 3% hydrogen peroxide for 10 min at room temperature to block endogenous peroxidase activity and 5% goat serum (Beijing Solarbio Science & Technology Co., Ltd.) for 30 min at 25°C to block non-specific binding sites. The sections were then incubated with the primary antibody anti-cyclin B1 (cat. no. TA374365; OriGene Technologies, Inc.) at a dilution of 1:300 overnight at 4°C. After warming for 1 h at room temperature, the sections were washed three times in PBS and then incubated with the undiluted secondary antibody goat anti-rabbit IgG-HRP (PV-9000; OriGene Technologies, Inc.) at 37°C for 20 min. The primary antibody was replaced with PBS to serve as the negative control. Finally, the sections were stained with DAB and imaged under a light microscope (DM3000; Leica Microsystems GmbH).

The IHC results were independently assessed by two experienced pathologists from Zunyi Medical University who were blinded to the clinical data of the patients. Five random fields from each section were observed under an optical microscope at x200 magnification. The expression of CCNB1 was scored according to the percentage of positive tumor cells and the staining intensity. The percentage of positive cells was scored according to the following criteria: 0 (0%), 1 (1-25%), 2 (26-50%), 3 (51-75%) and 4 (76-100%). The staining intensity was scored as follows: 0 (no staining), 1 (light yellow), 2 (brownish) and 3 (tan). The staining intensity score and the percentage of positive staining were summed to obtain the final score, with a total score >2 defined as positive expression and \leq 2 defined as negative expression.

Cell culture and transfection. The PC9, A549, H1299 and H827 LUAD cell lines were purchased from the Cell Bank of Type Culture Collection of the Chinese Academy of Sciences, and stored in the Cancer Research Laboratory of the Affiliated Hospital of Zunyi Medical University. The cells were cultured in RPMI-1640 (HyClone; Cytiva) supplemented with 10% fetal bovine serum (Shanghai XP Biomed Ltd.) and 100X Penicillin-Streptomycin Solution (Sangon Biotech Co., Ltd.) at 37°C with 5% CO₂. Small interfering RNAs (siRNAs) purchased from Sangon Biotech Co., Ltd. were used to knock down CCNB1. The sequences were as follows: CCNB1-PLVT7 forward, CTTGAGTTG GAGTACTATATT and reverse, AATATAGTACTCCAA CTCAAG; CCNB1-PLVT8 forward, GGTTGTTGCAGG AGACCATGT and reverse, ACATGGTCTCCTGCAACA ACC; CCNB1-PLVT9 forward, GATCGGTTTCATGCAG AATAAT and reverse, ATTATTCTGCATGAACCGATC; negative-PLVT forward, TTCTCCGAACGTGTCACGT and reverse, ACGTGACACGTTCCGAGAA. Cells were transfected with siRNAs targeting CCNB1 or non-sense control siRNA using Lipofectamine 2000 (Thermo Fisher Scientific, Inc.) according to the manufacturer's instructions. Briefly, the LUAD cells were seeded at a density of 1.5×10^5 in a 6-well

plate. Lipofectamine 2000 (Thermo Fisher Scientific, Inc.) was used to transfect the siRNAs into H1299 cell lines to select the most efficient one for subsequent use (CCNB1-PLVT7, CCNB1-PLVT8, CCNB1-PLVT9). Following the standard protocol, siR-NC or siR-CCNB1 (100 pmol/well; Shanghai GeneChem Co., Ltd.) was transfected into H1299 cell lines. After 6 h of culture at 37°C, the medium was replaced with DMEM containing 10% FBS. After cultivation for 72 h at 37°C, the cells were collected for further assays.

Reverse transcription-quantitative polymerase chain reaction (RT-qPCR). Total RNA was extracted from LUAD cells using RNAiso Plus reagent (Takara Bio, Inc.) according to the manufacturer's protocol, and cDNAs were reverse transcribed using a PrimeScript™ RT reagent Kit (Perfect Real Time) (Takara Bio, Inc.) at 37°C for 15 min. qPCR was performed with an ABI Prism 7500 Real-Time PCR system (Applied Biosystems; Thermo Fisher Scientific, Inc.) and a ChamQ™ Universal SYBR qPCR Master Mix Kit (Vazyme Biotech Co., Ltd.) was used to quantify the expression of CCNB1 and GAPDH. qPCR was initiated at 95°C for 3 min, followed by 40 cycles at 95°C for 20 sec and 60°C for 30 sec. GAPDH expression was used as the internal control, and the relative quantification of gene expression was calculated using the 2^{- $\Delta\Delta$ C_q} method (22). The primers were designed and synthesized by Sangon Biotech Co., Ltd. and their sequences were as follows: CCNB1 forward, 5'-GGAGAGCATCTAAGATTGGAGAGGTTG-3' and reverse, 5'-GCTTCGATGTGGCATACTTGTCTCTTG-3'; and β -actin forward, 5'-CCTGGCACCCAGCACAAAT-3' and reverse, 5'-GGGCCGGACTCGTCATAC-3'.

RNA extraction and RNA-seq. Total RNA was extracted from the LUAD cells using RNAiso Plus reagent (Takara Bio, Inc.) according to the manufacturer's protocol. Samples with RNA an optical density ratio 260 and 280 nm of >1.8 were subjected to subsequent analyses. Libraries were constructed using the TruSeq Stranded mRNA LT Sample Prep Kit (Illumina®; cat. no. RS-122-2101.) according to the manufacturer's instructions. The loading concentration of 30 ng/ μ l was measured by library quantification using Thermo Fisher Qubit Flex (Thermo Fisher Scientific, Inc.), and then the library was sequenced with a NovaSeq 6000 S4 Rgt Kit (20028312) on an Illumina sequencing platform (NovaSeq 6000; Illumina, Inc.), and 150 bp paired-end reads were generated. Base calling was performed with RTA v2.7.6 (Illumina, Inc.), and the fastq files were generated by bcl2fastq v2.15.0 (Illumina, Inc.). Removal of low-quality bases and adapters from paired-end reads was processed by fastp v0.22.0 (<https://github.com/OpenGene/fastp>). Alignment of the trimmed RNA-seq reads to the ensembl human genome assembly (GRCh38.p13; https://www.ensembl.org/Homo_sapiens/Info/Index) employed HISAT2 v2.2 (<http://daehwankimlab.github.io/hisat2/>). 1 with the options of '-k 3 -p 20 --pen-noncansplice 1000000'. The counts of the reads mapped to individual genes were calculated by featureCounts v2.0.3 (<http://subread.sourceforge.net/featureCounts.html>). DEGs were identified by the DESeq2 (version 3.15; <https://bioconductor.org/packages/DESeq2/>), a cut-off of padj <0.05 and $\log_2(\text{fold change}) > 1.5$ was applied.

Statistical analysis. The datasets were mainly analyzed using R package software (version 3.6.0; <https://www.r-project.org/>) and integrated using Perl (version 5.30.0.1; <https://strawberryperl.com/>). Tools for the analysis and interpretation of high-throughput genomic data were obtained from Bioconductor (version 3.15; <http://bioconductor.org/>). For normally distributed continuous variables, significant differences were detected using unpaired t-tests when two groups were compared and one-way ANOVA followed by Tukey's or Dunnett's post hoc tests when multiple groups were compared. For categorical variables, including the associations between CCNB1 and clinicopathological variables, analyses were performed using Pearson's χ^2 and Fisher's exact tests. The survival analysis was performed using Kaplan-Meier curves, and the significance of differences in survival was examined using the log-rank test. The Cox proportional hazards regression model was used for univariate and multivariate analyses. The hazard ratio (HR) and 95% confidence interval (CI) were calculated to estimate the hazard risk of variables. $P < 0.05$ was considered to indicate a statistically significant result.

Results

Expression of CCNB1 is higher in LUAD tissues than in normal lung tissues. To investigate the expression of CCNB1 in LUAD, data from the TCGA and GEO databases were analyzed. The mRNA expression of CCNB1 was significantly increased in LUAD tissues compared with normal lung tissues in both datasets ($P < 0.05$; Fig. 1A and B). In addition, LUAD tissues were collected from 94 patients undergoing surgical resection and 30 normal lung tissues were acquired for comparison. To verify that the expression of CCNB1 was higher in LUAD tissues than in normal lung tissues, the expression levels of CCNB1 in LUAD and normal tissues were detected using IHC. The IHC staining showed that CCNB1 was localized in the nucleus and cytoplasm (Fig. 1C). CCNB1 staining was negative in all 30 normal lung tissues, and among the 94 LUAD tissues, the positive expression of CCNB1 was detected in 27.66% (26/94) of patients. The frequency of positive expression of CCNB1 in LUAD was significantly higher than that in normal tissues ($P < 0.05$; Table I). These results suggest that CCNB1 is significantly upregulated in LUAD tissues compared with normal lung tissues.

Relationship between CCNB1 expression and the prognosis of patients with LUAD. The prognostic value of CCNB1 was assessed using TCGA-LUAD data. Kaplan-Meier survival curves were plotted to evaluate the relationship between CCNB1 and the prognosis of patients with LUAD. As shown in Fig. 2A, the OS significantly differed between the CCNB1-high and CCNB1-low patients ($P < 0.05$). Furthermore, this conclusion was validated by the primary patient data. Patients with positive CCNB1 expression had a worse prognosis than patients with negative CCNB1 expression ($P < 0.05$; Fig. 2B). To further analyze the prognostic value of CCNB1 expression in subgroups of patients, stratification by age, sex, smoking status, tumor size, lymph node status, pleural invasion status and clinical stage was performed. Kaplan-Meier analysis revealed that patients with CCNB1-positive results had a significantly shorter OS than patients with negative CCNB1

Table I. Expression of cyclin B1 in primary lung adenocarcinoma and normal lung tissues.

Group	N	Expression (n)		χ^2	P-value
		Negative	Positive		
Cancer	94	68	26	10.499	0.001
Normal	30	30	0		

expression in the T3 + T4 and N0 + N1 subgroups ($P < 0.05$; Fig. 2C and D, respectively). Univariate analysis suggested that patient survival was influenced by T stage, N state, stage and CCNB1 expression (Fig. 3A). Furthermore, multivariate analysis indicated that CCNB1 expression is an independent prognostic factor in patients with LUAD (Fig. 3B).

Association of CCNB1 expression with the clinicopathological parameters of patients with LUAD. The relationship between CCNB1 expression levels and the clinicopathological parameters of 334 patients in the TCGA-LUAD dataset were investigated. As shown in Fig. 4A, no significant difference in CCNB1 expression levels between stages I, II, III and IV was detected. Following this, the expression of CCNB1 in patients with different TNM stages was also compared, and no differences were identified (Fig. 4B-D). These results were consistent with the primary data collected from 94 patients. The associations between the CCNB1 expression levels and clinicopathological features of the patients are summarized in Table II. The results revealed no significant association between CCNB1 expression and clinical parameters, including age, sex, smoking, differentiation, bronchial margin, tumor size, lymph node metastasis, distant metastasis, T stage, pathological stage, visceral pleural invasion and tumor type.

RNA sequencing of H1299 cells with CCNB1 knockdown. To detect the expression level of CCNB1 *in vitro*, four LUAD cell lines, namely A549, H827, H1299 and PC9, were analyzed. The RT-qPCR results suggested that CCNB1 expression in H1299 cells was higher than that in the other three cell lines (Fig. 5A); therefore, H1299 cells were selected for subsequent experiments. To explore the specific mechanism of CCNB1 in LUAD, CCNB1 expression was knocked down using siRNAs in H1299 cells. Among the three CCNB1 siRNAs, CCNB1-PLVT7 was the most effective in knocking down CCNB1 at the mRNA level (Fig. 5B). Therefore, RNA-seq was performed on H1299 cells transfected with CCNB1-PLVT7 as the experimental group and transfected with PLVT7-mock as the control group, using three repeat samples for each group. The RNAs that underwent changes in expression in H1299 cells with CCNB1 knockdown were analyzed, and 135 DEGs in total were identified. By setting $\log_2(\text{fold change}) > 1.5$ as the upregulated threshold and < -1.5 as the downregulated threshold, 76 upregulated genes and 59 downregulated genes were detected (Fig. 5C). To explore the underlying biological functions of CCNB1 downregulation in LUAD, GO and KEGG enrichment analyses were performed on the 135 genes. The results of KEGG pathway analysis indicated that DEGs

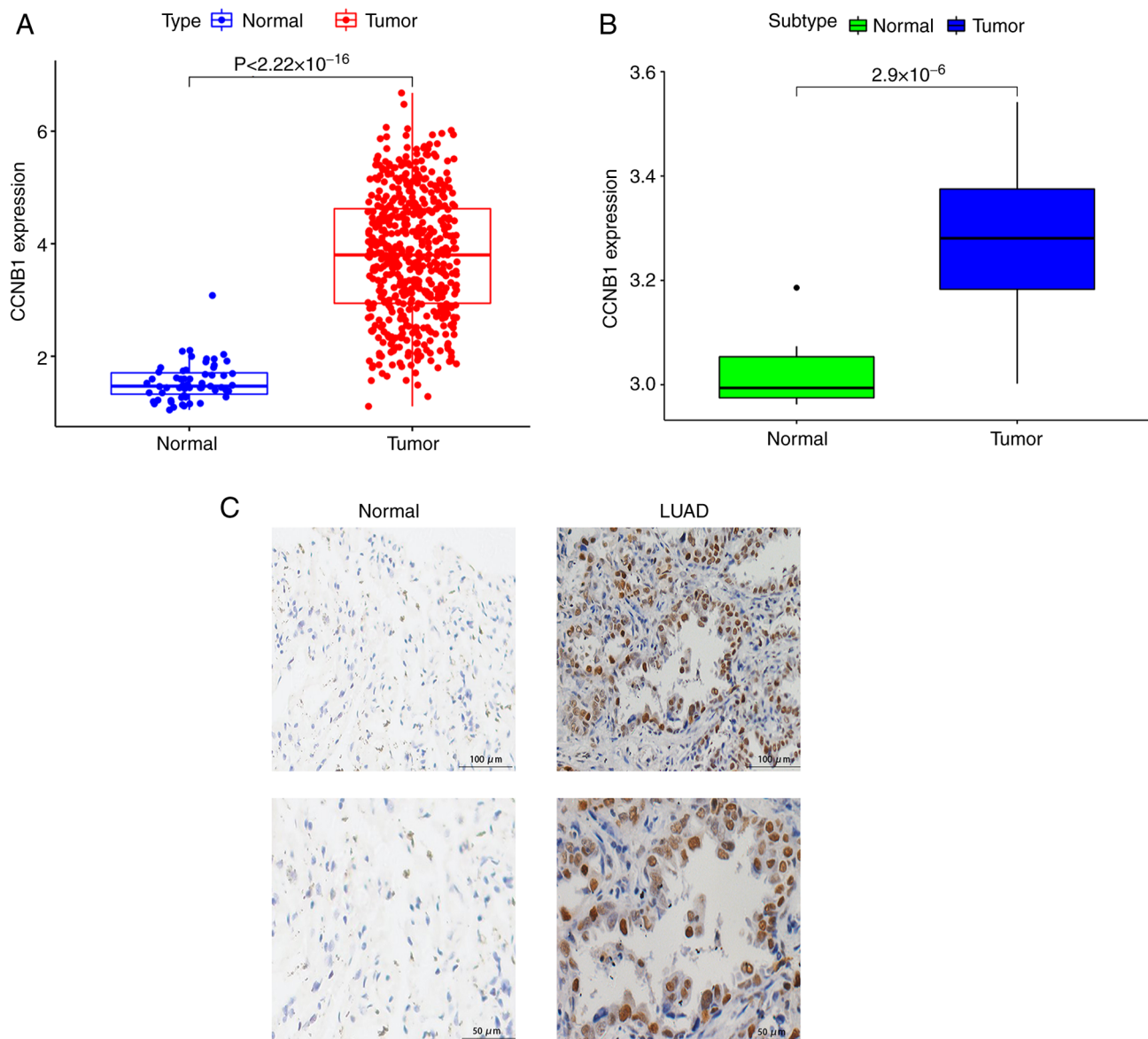


Figure 1. CCNB1 expression is significantly increased in LUAD tissues compared with normal lung tissues. (A) CCNB1 expression in 334 LUAD samples and 59 normal lung tissues from The Cancer Genome Atlas database. (B) CCNB1 expression in 57 LUAD samples and 11 normal lung tissues from GSE116959 of the Gene Expression Omnibus database. (C) Representative image of CCNB1 expression in the LUAD tissues of a patient at the Affiliated Hospital of Zunyi Medical University and normal lung tissues (upper image magnification, x200; lower image magnification, x400) detected using immunohistochemistry. CCNB1, cyclin B1; LUAD, lung adenocarcinoma.

were mainly enriched in ‘human papillomavirus infection’, ‘proteoglycans in cancer’, ‘regulation of actin cytoskeleton’, ‘focal adhesion’ and the ‘apelin signaling pathway’ (Fig. 5D). In addition, the results of GO enrichment analysis showed that the BP of the DEGs included ‘regulation of supramolecular fiber organization’, ‘regulation of actin filament organization’, ‘regulation of cellular component size’ and ‘regulation of cytoskeleton organization’ (Fig. 5E). The main CC biological processes included ‘focal adhesion’, ‘cell-substrate adherens junction’ and ‘cell-cell junction’ (Fig. 5E). The main MFs of the DEGs were ‘Ras GTPase binding’, ‘R-SMAD binding’, ‘fibronectin binding’ and ‘small GTPase binding’ (Fig. 5E).

Identification of co-expressed genes based on WGCNA and RNA-seq. CCNB1 has been shown to interact with other genes to promote the occurrence and development of tumors (23).

Therefore, to further study the interaction between the DEGs identified in the present study, cluster analysis was performed. A total of 5,756 DEGs were screened from the TCGA-LUAD dataset and are represented as a volcano plot (Fig. 6A). Co-expression analysis was carried out to construct a co-expression network. A power of $\beta=5$ was selected as the soft-thresholding parameter to ensure a scale-free network (Fig. 6B and C). A total of 7 modules were identified via average linkage hierarchical clustering (Fig. 6D). The 850 genes contained in the blue module had the highest association with CCNB1 expression. Comparison of the RNA-seq and WGCNA data led to the identification of six common genes: Complexin 1 (CPLX1), peptidylprolyl isomerase F (PPIF), serine-arginine protein kinase 2 (SRPK2), keratin 8 (KRT8), solute carrier family member 20 member 1 (SLC20A1) and chromobox 2 (CBX2) (Fig. 7A). Kaplan-Meier survival curves

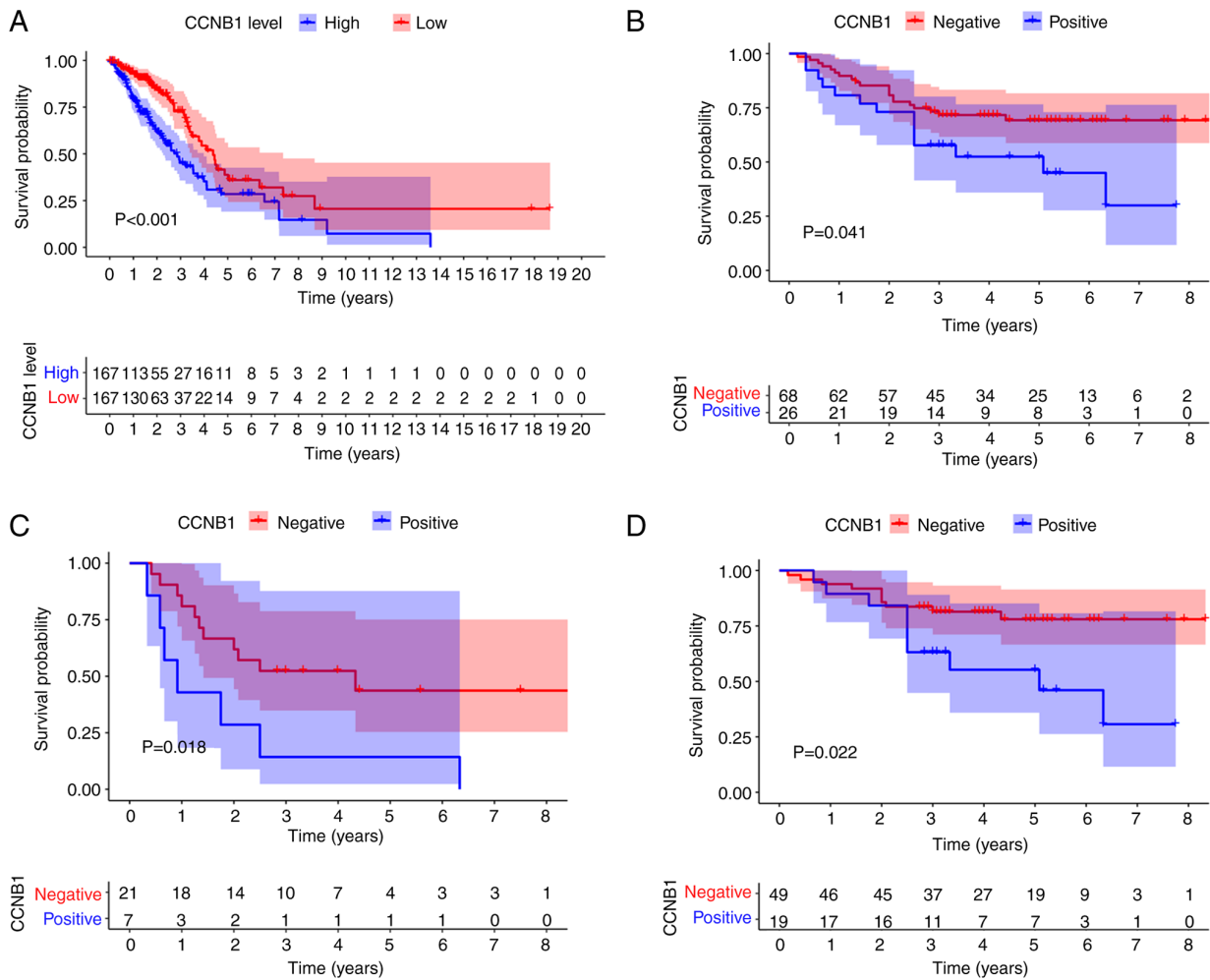


Figure 2. Association between CCNB1 expression and the prognosis of patients with lung adenocarcinoma. (A) Patients with high CCNB1 expression had a significantly shorter OS than patients with low CCNB1 expression according to data from The Cancer Genome Atlas database. (B) Patients with positive CCNB1 expression had a worse prognosis than patients with negative CCNB1 expression according to data from the Affiliated Hospital of Zunyi Medical University. Patients with positive CCNB1 expression had a significantly shorter OS than patients with negative CCNB1 expression when (C) T3 + T4 and (D) N0 + N1 cases were considered. CCNB1, cyclin B1; OS, overall survival.

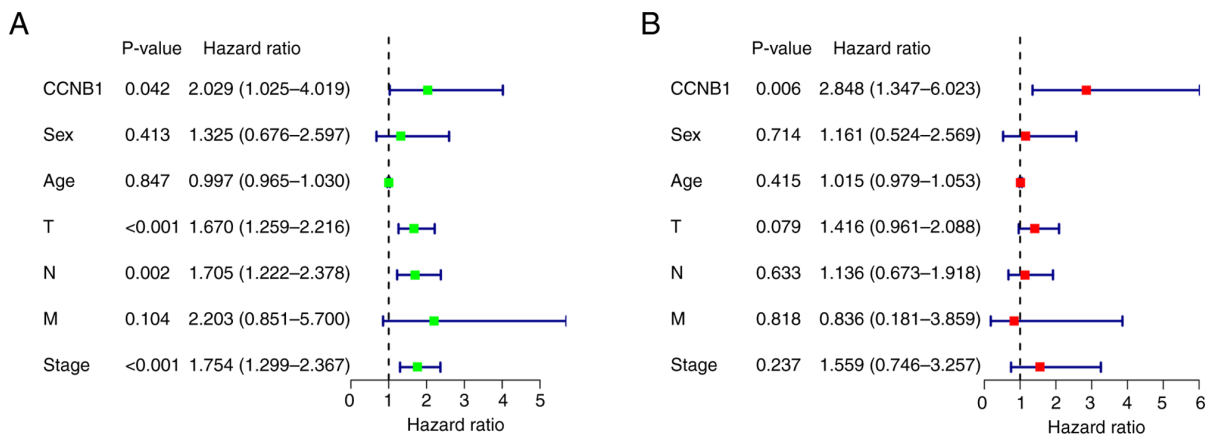


Figure 3. Univariate and multivariate Cox analysis of OS in 94 patients with lung adenocarcinoma from the Affiliated Hospital of Zunyi Medical University. (A) Univariate analysis suggested that patient survival was influenced by T, N, pathological stage and CCNB1. (B) Multivariate analysis showed that CCNB1 expression is an independent prognostic factor. CCNB1, cyclin B1.

were plotted for the 334 patients in the TCGA-LUAD dataset to evaluate the relationship between these genes and the prognosis of patients with LUAD. As shown in Fig. 7B and C, high

KRT8 or PPIF expression levels were unfavorable to the OS of patients with LUAD ($P < 0.05$), while the other four genes had no effect on prognosis (data not shown). These results indicate

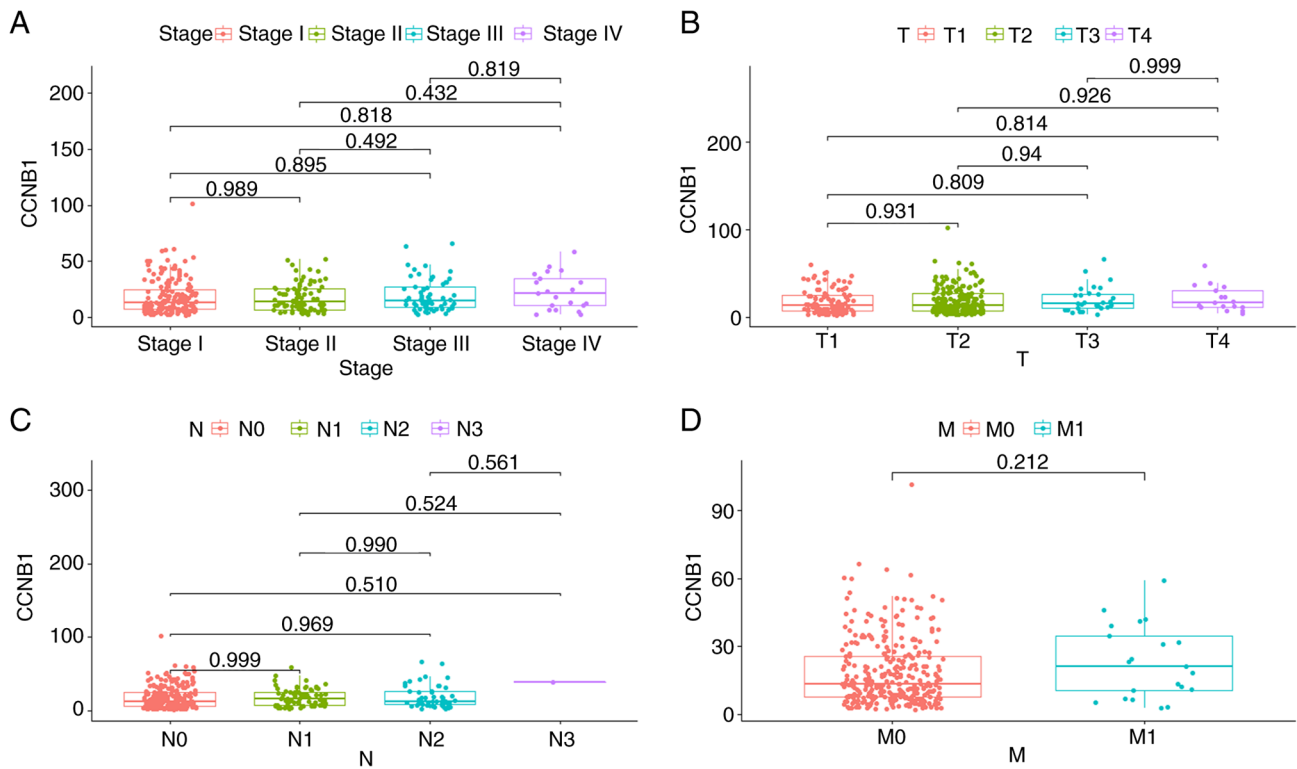


Figure 4. Comparison of CCNB1 expression in different clinicopathological groups from The Cancer Genome Atlas. Groups were analyzed according to (A) stage, (B) T stage, (C) N stage and (D) M stage. One-way ANOVA followed by Tukey's post hoc test was used to analyse the data in (A-C) and unpaired Student's t-test was used to analyse the data in (D). No significant differences were identified in stage or TNM stage. CCNB1, cyclin B1.

that CCNB1, as an independent prognostic factor of LUAD, may interact with CPLX1, PPIF, SRPK2, KRT8, SLC20A1 and CBX2 to influence the outcome of patients with LUAD.

Discussion

In the present study, clinical samples and bioinformatics methods were used to show that CCNB1 is highly expressed in LUAD tissues. Kaplan-Meier survival curves and multivariate Cox regression analysis confirmed that CCNB1 is an independent prognostic factor for patients with LUAD. Higher CCNB1 expression predicted worse overall survival, indicating that CCNB1 is an oncogene. However, CCNB1 expression was not found to be associated with any clinicopathological parameters. Integration of the results of RNA-seq and WGCNA analyses to identify intersecting genes indicated that CCNB1 may cooperate with CPLX1, PPIF, SRPK2, KRT8, SLC20A1 and CBX2 to affect the prognosis of patients with LUAD. In addition, GO and KEGG pathway analyses showed that a reduction in CCNB1 expression induces changes in different pathways.

Although the exact mechanism of CCNB1 upregulation is unclear, CCNB1 is known to be essential for the survival and proliferation of tumor cells; upregulated CCNB1 binds to its partner CDKs and promotes cancer cell growth (24). High levels of CCNB1 are associated with the immortalization of tumor cells and chromosomal instability, which contribute to tumor cell invasion and the prognosis of patients with cancer (25). Conversely, the decreased expression of CCNB1 causes tumor cell death (26). Downregulation of the expression of CCNB1 has

been shown to activate the p53 signaling pathway and thereby inhibit HCC cell growth (27). Although the role of CCNB1 has been reported in several types of cancer (28-32), its involvement in LUAD has not been elucidated. In the present study it was found that CCNB1 expression was significantly upregulated in LUAD tissues. These results suggest that CCNB1 may be involved in promoting the transformation of normal tissues into cancerous tissues and could be a cancer promoter. Kaplan-Meier survival analyses showed that patients with high CCNB1 expression had worse OS than those with low CCNB1 expression, which is consistent with previous reports of CCNB1 in hypopharyngeal squamous cell carcinoma (11), liver cancer (12,33) and oesophageal cancer (34). However, Chae *et al* (35) did not detect any association of the expression of CCNB1 with the prognosis of patients with breast cancer. These inconsistent findings could potentially be explained by the different expression patterns of CCNB1 in different types of tumors.

Furthermore, the associations between CCNB1 expression and clinicopathological parameters were analyzed in the present study using TCGA data and the immunohistochemical results of 94 patients with LUAD. However, as there were no positive findings, CCNB1 appears to be a relatively independent expression factor. Similar findings have been reported in previous studies on breast cancer (35), pediatric embryonic tumors (11) and pancreatic cancer (36). However, some studies have identified associations between CCNB1 and clinical factors in LUAD. For example Wang *et al* (18) found that CCNB1 expression level was clinically associated with sex, smoking, T stage and N stage in institutional and TCGA NSCLC cohorts. Furthermore, Bao *et al* (19) determined

Table II. Association of cyclin B1 expression with clinicopathological features in patients with lung adenocarcinoma.

Feature	N	CCNB1 expression (n)		P-value
		Negative	Positive	
Age				0.521
≤55	42	29	13	
>55	52	39	13	
Sex				0.367
Female	54	41	13	
Male	40	27	13	
Smoking				0.478
Yes	38	29	9	
No	56	39	17	
Tumor size (cm)				0.775
≤3.5	60	44	16	
>3.5 cm	34	24	10	
Differentiation				0.112
Low/moderate	49	32	17	
High	45	36	9	
T stage				0.707
T1 + T2	66	47	19	
T3 + T4	28	21	7	
Lymph node metastasis				0.484
Yes	31	21	10	
No	63	47	16	
Distant metastasis				0.704 ^a
Yes	9	6	3	
No	85	62	23	
Pathological stage				0.912
I + II	57	41	16	
III + IV	37	27	10	
Visceral pleural invasion				0.961
No	51	37	14	
Yes	43	31	12	
Bronchial margin				0.732 ^a
Positive	12	8	4	
Negative	82	60	22	
Tumor type				1.000 ^a
Central	11	8	3	
Peripheral	83	60	23	

^aFisher's exact test. Other features were analyzed using χ^2 . CCNB1, cyclin B1.

the expression of CCNB1 mRNA in patient tissues using RT-qPCR, which demonstrated that CCNB1 expression was high in LUAD tissues and associated with advanced tumor stages and shorter overall survival. However, in the present study, immunohistochemistry was used to detect CCNB1 protein expression, and the results may differ according to the experimental methods used. It is necessary to further expand the sample size and continue to explore the effect of CCNB1 on the clinicopathological factors of LUAD in future studies.

The mechanism of CCNB1 in LUAD was further explored in the present study by knocking down the expression of CCNB1 in H1299 cells and performing RNA-seq to detect the changes in gene expression at the transcriptional level. The GO and KEGG analysis results showed that the knock-down of CCNB1 caused changes in pathways associated with cytoskeleton-related proteins, the formation of focal adhesions, Ras GTPase binding and small GTPase binding. The increased expression of focal adhesion-associated

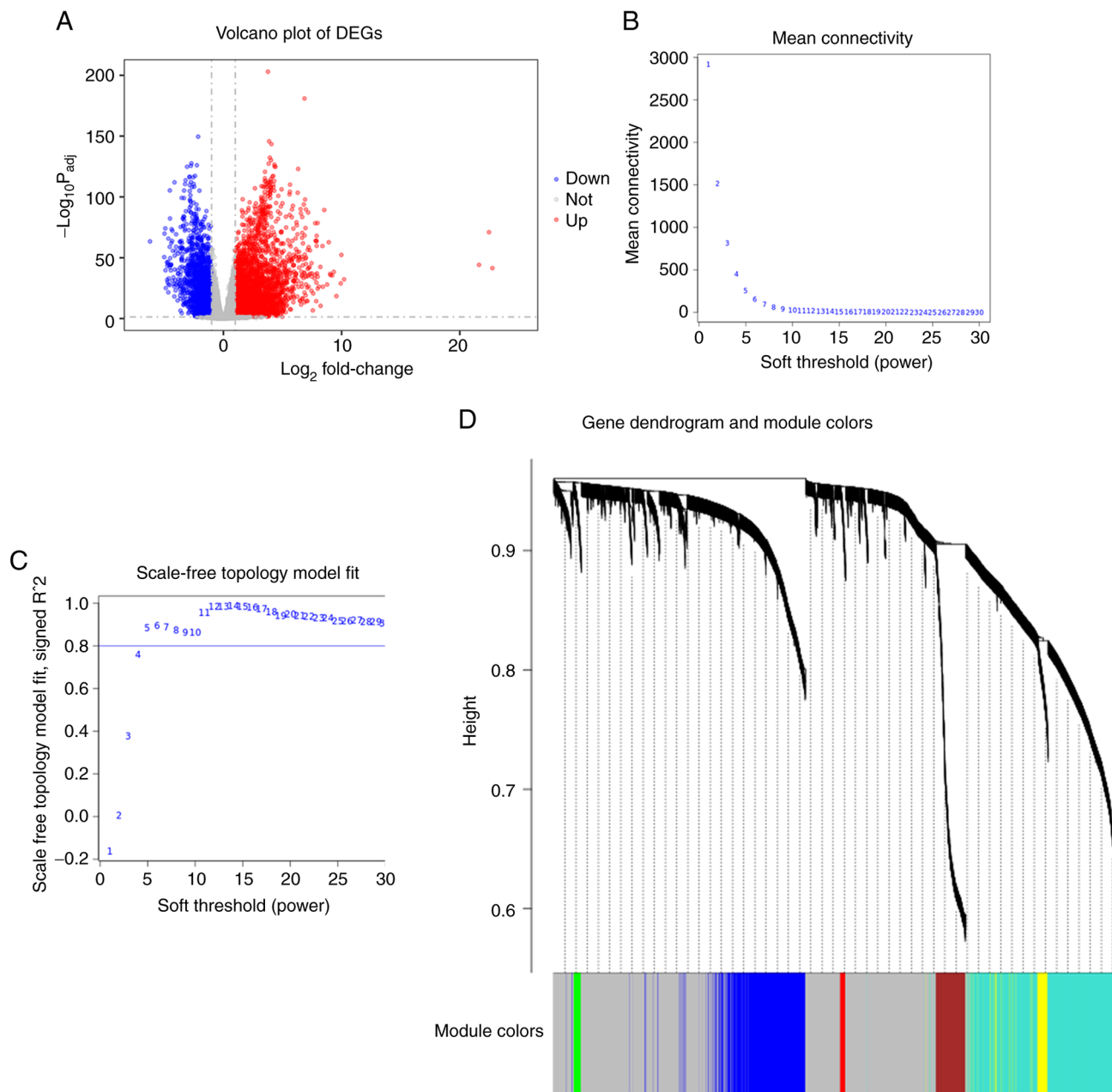


Figure 6. Identification of modules associate with cyclin B1. (A) Volcano plot of DEGs. (B) Analysis of the mean connectivity for soft-thresholding powers. (C) Analysis of the scale-free fit index for various soft-thresholding powers (β). (D) Dendrogram of all clusters based on a dissimilarity measure. DEGs, differentially expressed genes.

adhesion molecule, namely focal adhesion kinase (FAK), also plays a key role in numerous signal transduction pathways associated with tumor proliferation, apoptosis, metastasis, invasion and angiogenesis, and so is a potential antitumor target (39). FAK is overexpressed in a variety of cancers and is closely associated with the occurrence and development of tumors (40). As a functional protein in the cytoplasm, it usually acts in a kinase-dependent manner (41). By studying the expression and distribution of key proteins in the integrin-FAK-Rho GTPase signaling pathway, Shen *et al.* (42) elucidated their relationship with the molecular mechanism of endothelial cell adhesion and migration; cell migration and FAK phosphorylation levels are closely associated with the regulation of Rho GTPase expression. Therefore, we

hypothesize that the high expression of CCNB1 regulates the formation of focal adhesions in LUAD, affects FAK phosphorylation and then activates the GTPase pathway, thereby affecting the invasion and migration ability of LUAD cells and ultimately affecting the prognosis of patients.

The WGCNA results obtained in the present study showed that 850 genes, including CCNB1, were co-expressed in LUAD. After identifying the intersecting RNA-seq and WGCNA results, it was found that the expression of CPLX1, PPIF, SRPK2, KRT8, SLC20A1 and CBX2 was closely associated with that of CCNB1. Notably, Kaplan-Meier analyses revealed that high expression of KRT8 and PPIF was associated with poor prognosis. Previous studies have shown the significant upregulation of KRT8 expression in various types

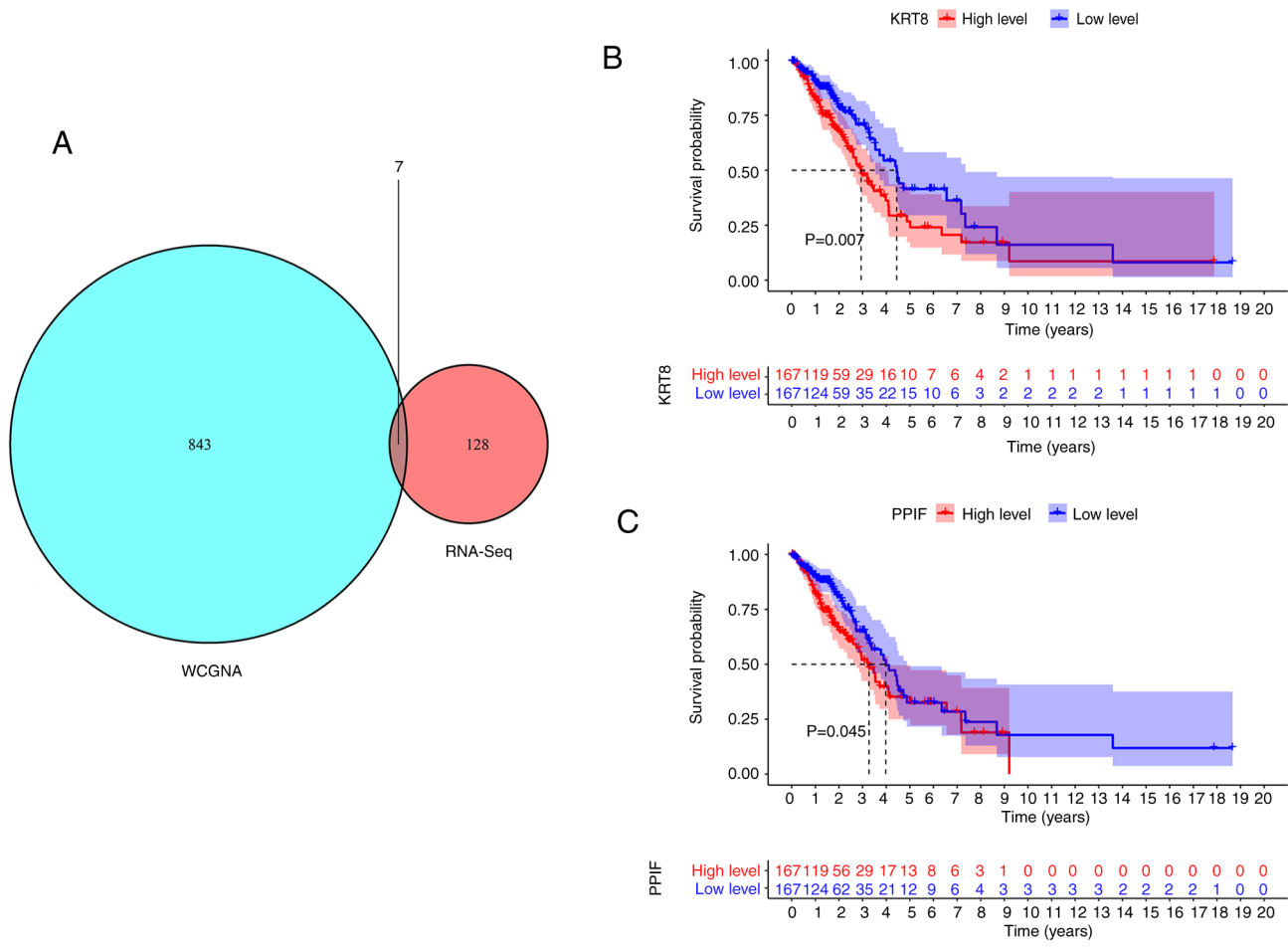


Figure 7. Co-expression analysis of CCNB1. (A) Venn diagram showing the co-expression of seven genes based on RNA-seq and WGCNA; KRT8, PPIF, complexin 1, serine-arginine protein kinase 2, solute carrier family member 20 member 1 and chromobox 2 were co-expressed with CCNB1. Kaplan-Meier analysis shows the association of (B) KRT8 and (C) PPIF with overall survival. CCNB1, cyclin B1; RNA-seq, RNA-sequencing; WGCNA, weighted gene co-expression network analysis; KRT8, keratin 8; PPIF, peptidylprolyl isomerase F.

of human cancer (43-45) and its predominant expression in epithelial cells. The aberrant expression of KRT8 in multiple types of tumors has been shown to be associated with cell migration (46), cell adhesion (47) and drug resistance (48). Other studies have reported that PPIF is involved in mitochondrial permeability transition-regulated necrosis and necroptosis (49,50), and strongly upregulated in endometrial cancer tissues with an expression profile closely associated with promoter hypomethylation (51). These data suggest that CPLX1, PPIF, SRPK2, KRT8, SLC20A1 and CBX2, particularly KRT8 and PPIF, are key genes involved in the biological effects of CCNB. However, the relationship between KRT8, PPIF and CCNB1 has not been reported in other related studies and is worthy of further exploration.

Interestingly, consistent results were obtained using TCGA data and clinical samples, both of which indicate that the increased expression of CCNB1 is a marker of poor prognosis for LUAD. Moreover, the findings suggest that CCNB1 may affect the expression of CPLX1, PPIF, SRPK2, KRT8, SLC20A1 and CBX2 genes, leading to a poor prognosis in patients with LUAD. This study provides a comprehensive and reliable theoretical basis and data source for subsequent studies of CCNB1 in LUAD. However, the study has certain limitations. Firstly, the sample size was

small and a larger sample size should be analyzed to further confirm the expression and prognostic value of CCNB1. Secondly, the mechanism merits further study, but no cell experiments were conducted to verify the potential mechanism. Further intensive *in vitro* and *in vivo* investigations should help to clarify the underlying mechanism of CCNB1 in the pathogenesis and development of LUAD. It is hoped that CCNB1 can be applied to the clinical practice of patients with LUAD to guide their prognosis and facilitate individualized treatment.

In conclusion, the present study identified that CCNB1 was highly expressed in patients with LUAD and associated with a poor prognosis. Patients whose IHC results were positive for CCNB1 expression had a significantly shorter OS than patients with whose results were negative. CCNB1 may affect the expression of the CPLX1, PPIF, SRPK2, KRT8, SLC20A1 and CBX2 genes and be functionally regulated by different pathways. CCNB1 has the potential to become a novel prognostic target for LUAD and may assist physicians in finding new diagnostic and therapeutic methods for patients with LUAD.

Acknowledgements

Not applicable.

Funding

This study was supported by the National Natural Science Foundation of China (grant nos. 81860469 and 82160574) and the Science and Technology Support Program of Guizhou [grant no. qiankehejichu (2020) 1Z063, qiankehezhicheng (2021 normal 073)].

Availability of data and materials

The datasets used and/or analyzed during the current study are available from the corresponding author on reasonable request. The raw sequencing datasets generated during the current study are available in the GEO repository (<https://www.ncbi.nlm.nih.gov/geo/query/acc.cgi?acc=GSE207450>).

Authors' contributions

YL, YXL, QL and CC conceived the project and participated in study design and interpretation of the results. YL wrote the manuscript. YXS, FC and YDD participated in study design and helped to revise the manuscript. YL and QYW contributed to sample collection and acquisition of patients' clinical and survival data. YXL, NJ and HD conducted experiments. YL and QL confirm the authenticity of all the raw data. All authors have read and approved the final manuscript.

Ethics approval and consent to participate

All experiments using human tissue were approved by the Ethics Committee of Zunyi Medical University [no. (2021)1-098]. Written informed consent was obtained from all patients for the use of their tissues in the study.

Patient consent for publication

Not applicable.

Competing interests

The authors declare that they have no competing interests.

References

- Siegel RL, Miller KD and Jemal A: Cancer statistics, 2020. *CA Cancer J Clin* 70: 7-30, 2020.
- Chen Z, Fillmore CM, Hammerman PS, Kim CF and Wong KK: Non-small-cell lung cancers: A heterogeneous set of diseases. *Nat Rev Cancer* 14: 535-546, 2014.
- Xia L, Zhu Y, Zhang C, Deng S, Deng Y, Yang Z, Mei J and Liu L: Decreased expression of EFCC1 and its prognostic value in lung adenocarcinoma. *Ann Transl Med* 7: 672, 2019.
- Macheleidt IF, Dalvi PS, Lim SY, Meemboor S, Meder L, Käsgen O, Müller M, Kleemann K, Wang L, Nurnberg P, *et al*: Preclinical studies reveal that LSD1 inhibition results in tumor growth arrest in lung adenocarcinoma independently of driver mutations. *Mol Oncol* 12: 1965-1979, 2018.
- Lim W, Bae H, Bazer FW and Song G: Ephrin A1 promotes proliferation of bovine endometrial cells with abundant expression of proliferating cell nuclear antigen and cyclin D1 changing the cell population at each stage of the cell cycle. *J Cell Physiol* 234: 4864-4873, 2019.
- Hydbring P, Malumbres M and Sicinski P: Non-canonical functions of cell cycle cyclins and cyclin-dependent kinases. *Nat Rev Mol Cell Biol* 17: 280-292, 2016.
- Braschi B, Denny P, Gray K, Jones T, Seal R, Tweedie S, Yates B and Bruford E: Genenames.org: The HGNC and VGNC resources in 2019. *Nucleic Acids Res* 47 (D1): D786-D792, 2019.
- Vishnoi N and Yao J: Single-cell, single-mRNA analysis of *Ccnb1* promoter regulation. *Sci Rep* 7: 2065, 2017.
- Liu D, Xu W, Ding X, Yang Y, Su B and Fei K: Polymorphisms of *CCNB1* associated with the clinical outcomes of platinum-based chemotherapy in Chinese NSCLC patients. *J Cancer* 8: 3785-3794, 2017.
- Wei LJ, Li JA, Bai DM and Song Y: miR-223-RhoB signaling pathway regulates the proliferation and apoptosis of colon adenocarcinoma. *Chem Biol Interact* 289: 9-14, 2018.
- Li W, Dong Q, Li L, Zhang Z, Cai X and Pan X: Prognostic significance of claudin-1 and cyclin B1 protein expression in patients with hypopharyngeal squamous cell carcinoma. *Oncol Lett* 11: 2995-3002, 2016.
- Chai N, Xie HH, Yin JP, Sa KD, Guo Y, Wang M, Liu J, Zhang XF, Zhang X, Yin H, *et al*: FOXM1 promotes proliferation in human hepatocellular carcinoma cells by transcriptional activation of *CCNB1*. *Biochem Biophys Res Commun* 500: 924-929, 2018.
- Gu J, Liu X, Li J and He Y: MicroRNA-144 inhibits cell proliferation, migration and invasion in human hepatocellular carcinoma by targeting *CCNB1*. *Cancer Cell Int* 19: 15, 2019.
- Fang Y, Liang X, Jiang W, Li J, Xu J and Cai X: Cyclin b1 suppresses colorectal cancer invasion and metastasis by regulating e-cadherin. *PLoS One* 10: e0126875, 2015.
- Sit M, Aktas G, Ozer B, Kocak MZ, Erkus E, Erkol H, Yaman S and Savli H: Mean platelet volume: An overlooked herald of malignant thyroid nodules. *Acta Clin Croat* 58: 417-420, 2019.
- Wang Y, Ruan Y and Wu S: ET-1 regulates the human umbilical vein endothelial cell cycle by adjusting the ER β /FOXN1 signaling pathway. *Ann Transl Med* 8: 1499, 2020.
- Brcic L, Heidinger M, Sever AZ, Zacharias M, Jakopovic M, Fediuk M, Maier A, Quehenberger F, Seiwerth S and Popper H: Prognostic value of cyclin A2 and B1 expression in lung carcinoids. *Pathology* 51: 481-486, 2019.
- Wang F, Chen X, Yu X and Lin Q: Degradation of *CCNB1* mediated by APC11 through UBA52 ubiquitination promotes cell cycle progression and proliferation of non-small cell lung cancer cells. *Am J Transl Res* 11: 7166-7185, 2019.
- Bao B, Yu X and Zheng W: MiR-139-5p targeting *CCNB1* modulates proliferation, migration, invasion and cell cycle in lung adenocarcinoma. *Mol Biotechnol* 64: 852-860, 2022.
- Leon LM, Gautier M, Allan R, Ilić M, Nottet N, Pons N, Paquet A, Lebrigand K, Truchi M, Fassy J, *et al*: Correction: The nuclear hypoxia-regulated *NLUCAT1* long non-coding RNA contributes to an aggressive phenotype in lung adenocarcinoma through regulation of oxidative stress. *Oncogene* 40: 2621, 2021.
- Aran D, Camarda R, Odegaard J, Paik H, Oskotsky B, Krings G, Goga A, Sirota M and Butte AJ: Comprehensive analysis of normal adjacent to tumor transcriptomes. *Nat Commun* 8: 1077, 2017.
- Livak KJ and Schmittgen TD: Analysis of relative gene expression data using real-time quantitative PCR and the 2(-Delta Delta C(T)) method. *Methods* 25: 402-408, 2001.
- Arora S, Singh P, Rahmani AH, Almatroodi SA, Dohare R and Syed MA: Unravelling the role of miR-20b-5p, *CCNB1*, *HMG A2* and *E2F7* in development and progression of non-small cell lung cancer (NSCLC). *Biology (Basel)* 9: 201, 2020.
- Fang L, Du WW, Awan FM, Dong J and Yang BB: The circular RNA circ-*Ccnb1* dissociates *Ccnb1/Cdk1* complex suppressing cell invasion and tumorigenesis. *Cancer Lett* 459: 216-226, 2019.
- Zhan Q, Antinore MJ, Wang XW, Carrier F, Smith ML, Harris CC and Fornace AJ Jr: Association with *Cdc2* and inhibition of *Cdc2/Cyclin B1* kinase activity by the p53-regulated protein *Gadd45*. *Oncogene* 18: 2892-2900, 1999.
- Vairapandi M, Balliet AG, Hoffman B and Liebermann DA: *GADD45b* and *GADD45g* are *cdc2/cyclinB1* kinase inhibitors with a role in S and G2/M cell cycle checkpoints induced by genotoxic stress. *J Cell Physiol* 192: 327-338, 2002.
- Li M, Shang H, Wang T, Yang SQ and Li L: Huanglian decoction suppresses the growth of hepatocellular carcinoma cells by reducing *CCNB1* expression. *World J Gastroenterol* 27: 939-958, 2021.
- Ding K, Li W, Zou Z, Zou X and Wang C: *CCNB1* is a prognostic biomarker for ER+ breast cancer. *Med Hypotheses* 83: 359-364, 2014.
- Chen EB, Qin X, Peng K, Li Q, Tang C, Wei YC, Yu S, Gan L and Liu TS: HnRNPR-*CCNB1*/CENPF axis contributes to gastric cancer proliferation and metastasis. *Aging (Albany NY)* 11: 7473-7491, 2019.

30. Moon SJ, Kim JH, Kong SH and Shin CS: Protein expression of cyclin B1, transferrin receptor, and fibronectin is correlated with the prognosis of adrenal cortical carcinoma. *Endocrinol Metab (Seoul)* 35: 132-141, 2020.
31. Xing Z, Wang X, Liu J, Zhang M, Feng K and Wang X: Expression and prognostic value of CDK1, CCNA2, and CCNB1 gene clusters in human breast cancer. *J Int Med Res* 49: 300060520980647, 2021.
32. Radhakrishnan A, Nanjappa V, Raja R, Sathe G, Chavan S, Nirujogi RS, Patil AH, Solanki H, Renuse S, Sahasrabudhe NA, *et al*: Dysregulation of splicing proteins in head and neck squamous cell carcinoma. *Cancer Biol Ther* 17: 219-229, 2016.
33. Zhuang L, Yang Z and Meng Z: Upregulation of BUB1B, CCNB1, CDC7, CDC20, and MCM3 in tumor tissues predicted worse overall survival and disease-free survival in hepatocellular carcinoma patients. *Biomed Res Int* 2018: 7897346, 2018.
34. Fu S, Jin L, Gong T, Pan S, Zheng S, Zhang X, Yang T, Sun Y, Wang Y, Guo J, *et al*: Effect of sinomenine hydrochloride on radiosensitivity of esophageal squamous cell carcinoma cells. *Oncol Rep* 39: 1601-1608, 2018.
35. Chae SW, Sohn JH, Kim DH, Choi YJ, Park YL, Kim K, Cho YH, Pyo JS and Kim JH: Overexpressions of cyclin B1, cdc2, p16 and p53 in human breast cancer: The clinicopathologic correlations and prognostic implications. *Yonsei Med J* 52: 445-453, 2011.
36. Zhou L, Li J, Zhao YP, Cui QC, Zhou WX, Guo JC, You L, Wu WM and Zhang TP: The prognostic value of cyclin B1 in pancreatic cancer. *Med Oncol* 31: 107, 2014.
37. Woldu SL, Hutchinson RC, Krabbe LM, Sanli O and Margulis V: The Rho GTPase signalling pathway in urothelial carcinoma. *Nat Rev Urol* 15: 83-91, 2018.
38. Lawson CD and Ridley AJ: Rho GTPase signaling complexes in cell migration and invasion. *J Cell Biol* 217: 447-457, 2018.
39. Zhou B, Wang GZ, Wen ZS, Zhou YC, Huang YC, Chen Y and Zhou GB: Somatic mutations and splicing variants of focal adhesion kinase in non-small cell lung cancer. *J Natl Cancer Inst* 110: 195-204, 2018.
40. Walker S, Foster F, Wood A, Owens T, Brennan K, Streuli CH and Gilmore AP: Oncogenic activation of FAK drives apoptosis suppression in a 3D-culture model of breast cancer initiation. *Oncotarget* 7: 70336-70352, 2016.
41. Brami-Cherrier K, Gervasi N, Arsenieva D, Walkiewicz K, Bouterin MC, Ortega A, Leonard PG, Seantier B, Gasmil L, Bouceba T, *et al*: FAK dimerization controls its kinase-dependent functions at focal adhesions. *EMBO J* 33: 356-370, 2014.
42. Shen Y, Ma Y, Gao M, Lai Y, Wang G, Yu Q, Cui FZ and Liu X: Integrins-FAK-Rho GTPases pathway in endothelial cells sense and response to surface wettability of plasma nanocoatings. *ACS Appl Mater Interfaces* 5: 5112-5121, 2013.
43. Selamat SA, Chung BS, Girard L, Zhang W, Zhang Y, Campan M, Siegmund KD, Koss MN, Hagen JA, Lam WL, *et al*: Genome-scale analysis of DNA methylation in lung adenocarcinoma and integration with mRNA expression. *Genome Res* 22: 1197-1211, 2012.
44. Sanchez-Carbayo M, Socci ND, Lozano J, Saint F and Cordon-Cardo C: Defining molecular profiles of poor outcome in patients with invasive bladder cancer using oligonucleotide microarrays. *J Clin Oncol* 24: 778-789, 2006.
45. Curtis C, Shah SP, Chin SF, Turashvili G, Rueda OM, Dunning MJ, Speed D, Lynch AG, Samarajiwa S, Yuan Y, *et al*: The genomic and transcriptomic architecture of 2,000 breast tumours reveals novel subgroups. *Nature* 486: 346-352, 2012.
46. Fortier AM, Asselin E and Cadrin M: Keratin 8 and 18 loss in epithelial cancer cells increases collective cell migration and cisplatin sensitivity through claudin1 up-regulation. *J Biol Chem* 288: 11555-11571, 2013.
47. Galarneau L, Loranger A, Gilbert S and Marceau N: Keratins modulate hepatic cell adhesion, size and G1/S transition. *Exp Cell Res* 313: 179-194, 2007.
48. Wang Y, He QY, Tsao SW, Cheung YH, Wong A and Chiu JF: Cytokeratin 8 silencing in human nasopharyngeal carcinoma cells leads to cisplatin sensitization. *Cancer Lett* 265: 188-196, 2008.
49. Mulay SR, Honarpisheh MM, Foresto-Neto O, Shi C, Desai J, Zhao ZB, Marschner JA, Popper B, Buhl EM, Boor P, *et al*: Mitochondria permeability transition versus necroptosis in oxalate-induced AKI. *J Am Soc Nephrol* 30: 1857-1869, 2019.
50. Nakagawa T, Shimizu S, Watanabe T, Yamaguchi O, Otsu K, Yamagata H, Inohara H, Kubo T and Tsujimoto Y: Cyclophilin D-dependent mitochondrial permeability transition regulates some necrotic but not apoptotic cell death. *Nature* 434: 652-658, 2005.
51. Yang L, Cui Y, Sun X and Wang Y: Overexpression of TICRR and PPIF confer poor prognosis in endometrial cancer identified by gene co-expression network analysis. *Aging (Albany NY)* 13: 4564-4589, 2021.



This work is licensed under a Creative Commons Attribution-NonCommercial-NoDerivatives 4.0 International (CC BY-NC-ND 4.0) License.